Numerical Investigation of Viscous Dissipation in Elliptic Microducts

2014 J. Phys.: Conf. Ser. 547 012023

(http://iopscience.iop.org/1742-6596/547/1/012023)

Journal of Physics: Conference Series **547** (2014) 012023 doi:10.1088/1742-6596/547/1/012023

Numerical Investigation of Viscous Dissipation in Elliptic Microducts

P Vocale[1], G Puccetti[2], GL Morini[2], M Spiga[1]

[1]Department of Industrial Engineering, University of Parma, Parco Area delle Scienze 181/A, 43124 Parma, Italy.

[2] DIN – Alma Mater Studiorum Università di Bologna, Laboratorio di Microfluidica, Via del Lazzaretto 15/5, Bologna 40131, Italy.

E-mail: pamela.vocale@unipr.it

Abstract. In this work a numerical analysis of heat transfer in elliptical microchannels heated at constant and uniform heat flux is presented. A gaseous flow has been considered, in laminar steady state condition, in hydrodynamically and thermally fully developed forced convection, accounting for the rarefaction effects. The velocity and temperature distributions have been determined in the elliptic cross section, for different values of aspect ratio, Knudsen number and Brinkman number, solving the Navier-Stokes and energy equations within the Comsol Multiphysics® environment. The numerical procedure has been validated resorting to data available in literature for slip flow in elliptic cross sections with Br =0 and for slip flow in circular ducts with Br >0. The comparison between numerical results and data available in literature shows a perfect agreement. The velocity and temperature distributions thus found have been used to calculate the average Nusselt number in the cross section. The numerical results for Nusselt number are presented in terms of rarefaction degree (Knudsen number), of viscous dissipation (Brinkman number), and of the aspect ratio. The results point out that the thermal fluid behavior is significantly affected by the viscous dissipation for low rarefaction degrees and for aspect ratios of the elliptic cross-section higher than 0.2.

1. Introduction

The tendency of increasing power rating in electronic systems requires advanced technology in thermal management, and the introduction of microchannels into power cooling has significantly increased the need of more refined models to determine the thermal performance.

Experimental results on single-phase flows in microchannels have evidenced that the conventional models, can no longer be considered able to predict pressure drop and convective heat transfer coefficients. Researchers justify this conclusion by invoking new micro-effects (such as viscous forces, rarefaction, compressibility, axial heat conduction, conjugate heat transfer, wall roughness and so on), which Herwig and Hausner [1] called “scaling effects with respect to a standard macro-analysis”. In the analysis of microchannels, scaling effects are of paramount importance to describe the behavior of the fluid.

With regards to the viscous forces, it is well-know that their influence on the heat transfer is significant for highly viscous fluids or for flows characterized by high velocity. However it has to be pointed out that the role of the viscous dissipation becomes significant also when the temperature

difference between the fluid and the wall is small and when the channel diameter is reduced (as it occurs in microscale) [2].

In the last years many researchers have investigated the combined effect of rarefaction and viscous dissipation on the fluid behavior in microducts featuring different cross-sections, as highlighted by Colin in a recent review [3]. In particular, the thermal problem in uniform heat flux (CHF) boundary conditions has been tackled by many researchers. By applying the integral transform technique, Tunc and Bayazitoglu [4] analytically investigated the influence of Knudsen number and Brinkman number on the convective heat transfer in microducts. They found that an increase in the Knudsen number leads to a decrease in the Nusselt number, due to the temperature jump. By including the contribution of the viscous dissipation, they observed that the Nusselt number decreases as the Brinkman number increases. It has to be pointed out that for CHF boundary conditions a positive value of the Brinkman number means that the fluid is being heated.

The same problem has been theoretically investigated by Aydın and Avcı [5]. They found that for low values of the Brinkman number the Nusselt number decreases as the Knudsen number increases, while *Nu* presents a maximum for high values of *Br*. Their results show also that the influence of the Brinkman number becomes less relevant as the rarefaction effects become more pronounced because of the presence of the slip velocity which reduces the velocity gradient. These results have been confirmed by the analysis carried out by Jeong and Jeong [6] and by Çetin et al. [7] who have investigated the effect of rarefaction, viscous dissipation and axial conduction in microtubes by extending the classical Graetz problem. The same trend has been also observed by Sun et al. [8] who have performed a numerical investigation on slip flow in microducts accounting for rarefaction and viscous dissipation effects. The influence of viscous dissipation and rarefaction in micropipes has been also investigated by Hooman [9] who has extended the analysis to the Second Law presenting correlations for the dimensionless entropy generation number and for the Bejan number depending on the Brinkman and Knudsen numbers.

Closed form solutions for temperature and Nusselt number have been derived by Sadeghi and Saidi [10] in a microannulus. They have also investigated the influence of viscous dissipation accounting for the rarefaction effects in microchannels bounded by parallel plate as well. The role of viscous forces in the latter geometry has been also analytically analyzed by Jeong and Jeong [11], Aydın and Avcı [12] and more recently by Zhang et al. [13].

Moreover the combined effect of viscous dissipation and rarefaction has been numerically investigated in other cross-section geometries, even considering uniform heat flux (CHF) boundary conditions. van Rij [14,15] and Sun and Jaluria [16] have analyzed convective heat transfer in rectangular microducts. Their results show that viscous heating significantly affects the fluid thermal behavior, leading to a decrease in the Nusselt number, when the fluid is being heated. The amount of this reduction depends on the rarefaction degree, the aspect ratio and on the value of the Brinkman number. The same conclusions have been stated by Kuddusi [17] who have performed a numerical investigation of slip flow in trapezoidal microchannels accounting for the viscous heating.

Despite these important contributions, the influence of the viscous and rarefaction effect in elliptic microducts has not yet been investigated in literature, at least to the best knowledge of the authors.

In this work convective heat transfer for a laminar and fully developed gaseous flow, through elliptical microchannels, is investigated by adopting a numerical approach. The momentum conservation and energy equations are solved within the Comsol Multiphysics® environment considering a constant and uniform heat flux and accounting for the rarefaction effects. The numerical procedure is validated by comparing the numerical results with the data available in literature for both elliptic and circular microducts. The numerical data for the Nusselt number are presented as a function of the main parameters that influence the fluid behavior, highlighting the role of the viscous forces, of the rarefaction degree and of the aspect ratio of the considered cross-section.

The main goal of this work is to demonstrate that the problem of heat transfer enhancement in microdevices cannot be solved simply by indefinitely reducing the microchannel dimensions, because

the viscous dissipation effects shall offset the gains of high heat transfer coefficients associated with a reduction in the channel size.

2. Mathematical model

Experimental investigations highlight that, within the slip flow regime, at a distance of approximately one mean free path from the wall the continuum hypothesis is still valid, hence the problem is commonly tackled using the Navier-Stokes and energy equations, but modifying the boundary conditions to account for the rarefaction effects in the channels. To represent these effects, Knudsen number, defined as the ratio of the molecular mean free path to the hydraulic diameter of the cross section, is invoked. According to Karniadakis et al. [18] a slip flow model can be used for $0.001<Kn<0.1$.

By considering a Newtonian gas flowing in an elliptical microchannel (Fig. 1) and assuming that the physical properties are constant and the flow is laminar and fully developed, the Navier-Stokes equation can be written as follows:

$$\mu\left(\frac{\partial^2 u}{\partial \xi^2}+\frac{\partial^2 u}{\partial \psi^2}\right)=\frac{\partial p}{\partial \zeta} \tag{1}$$

being μ, u and $\partial p/\partial \zeta$, the fluid dynamic viscosity, the local velocity and the axial component of the pressure gradient, respectively. Due to low value of the Mach number, in the present analysis the compressibility effects are not considered [19].

The temperature field can be found by the solution of the energy equation:

$$\rho c_p u\frac{\partial T}{\partial \zeta}=\lambda\left(\frac{\partial^2 T}{\partial \xi^2}+\frac{\partial^2 T}{\partial \psi^2}\right)+\Phi \tag{2}$$

being ρ and λ the fluid density and thermal conductivity, respectively, and c_p the specific heat at constant pressure. The last term in Equation (2) indicates the viscous dissipation function which is defined by:

$$\Phi=\mu\left[\left(\frac{\partial u}{\partial \xi}\right)^2+\left(\frac{\partial u}{\partial \psi}\right)^2\right] \tag{3}$$

In fully developed flow, $dT_b/d\zeta=\partial T/\partial \zeta$, therefore the axial component of the temperature gradient can be evaluated by an overall energy balance for an elemental control volume:

$$\rho c_p WA\frac{\partial T}{\partial \zeta}=qL_P+\int_A \Phi dA \tag{4}$$

where W is the average fluid velocity, A indicates the cross-sectional area, q the wall heat flux and L_P the heated perimeter of the cross-section.

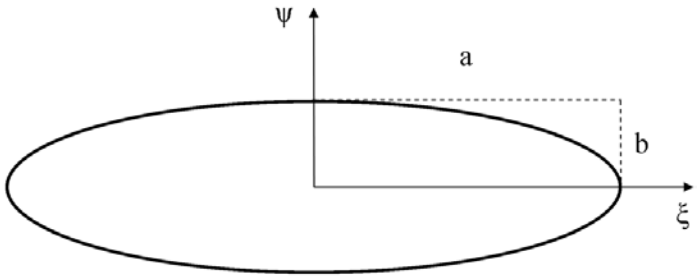

Figure 1. Sketch of the considered cross-section.

To obtain a general solution for the considered model, the following dimensionless coordinates are introduced:

$$x = \frac{\xi}{D_h} \qquad y = \frac{\psi}{D_h} \qquad z = \frac{\zeta}{D_h} \tag{5}$$

together with the dimensionless functions listed below:

$$P = -\frac{{D_h}^2}{\mu W}\frac{\partial p}{\partial \zeta} \qquad U = \frac{u}{W} \qquad \theta = \frac{\lambda T}{q\, D_h} \tag{6}$$

By considering the above non-dimensional quantities, the Equations (1-2) can be rewritten as follow:

$$\frac{\partial^2 U}{\partial x^2} + \frac{\partial^2 U}{\partial y^2} = P \tag{7}$$

$$\frac{\partial^2 \theta}{\partial x^2} + \frac{\partial^2 \theta}{\partial y^2} = \frac{U}{A^*}\left[L_P{}^* + Br \int_{A^*} \Phi^* dA^* \right] - Br\Phi^* \tag{8}$$

in which A^* denotes the dimensionless cross-sectional area ($A^*=A/{D_h}^2$), $L_P{}^*$ is the dimensionless heated perimeter of the cross-section ($L_P{}^*=L_P/D_h$), and Br indicates the Brinkman number defined by:

$$Br = \frac{\mu W^2}{q D_h} \tag{9}$$

To take into account the rarefaction effects, for the dimensionless velocity at the wall the usual first-order slip boundary condition is considered, according to [20]:

$$U - U_w = \frac{2-\sigma_v}{\sigma_v} Kn \left(\frac{\partial U}{\partial n} \right)_w \tag{10}$$

The energy equation is solved by considering a constant and uniform heat flux at the wall (i.e. H2 boundary conditions), hence the thermal boundary condition in the non-dimensional form reads as:

$$\left(\frac{\partial \theta}{\partial n} \right)_w = -1 \tag{11}$$

By considering the temperature jump at the wall, the non-dimensional wall temperature can be evaluated as follows:

$$\theta_w(x_w, y_w) = \theta(x_w, y_w) + \frac{2-\sigma_T}{\sigma_T} \frac{2k}{k+1} \frac{Kn}{\mathrm{Pr}} \tag{12}$$

The knowledge of the velocity and temperature fields enables to calculate the main physical parameters, such as the dimensionless bulk temperature and the average Nusselt number:

$$\theta_b = \frac{1}{A^*} \int_{A^*} U \theta dA^* \tag{13}$$

$$Nu = \frac{h\, D_h}{\lambda} = \frac{1}{(\overline{\theta_w} - \theta_b)} \tag{14}$$

in which $\overline{\theta_w}$ indicates the non-dimensional average wall temperature.

3. Results and discussion

The Navier-Stokes and energy equations in the non-dimensional form have been solved within the COMSOL Multiphysics® environment. To guarantee accurate solutions for the governing equations the convergence criterion has been set 1e-06.

The numerical runs have been performed considering air as working fluid (Pr=0.7, k=1.4) and assuming accommodation coefficients $\sigma_v = \sigma_T = 1$, as usual in literature [3].

To obtain mesh-independent solutions, several numerical simulations have been carried out on different grid sizes by monitoring the value of the Nusselt number. For each analysed grid resolution the relative error in Nu has been calculated by comparing the value of Nusselt number for the tested mesh size with a reference value of Nu obtained adopting the finest mesh (i.e. for each value of the aspect ratio considered in the present study a reference grid characterized by at least 400000 elements has been chosen):

$$\varepsilon_r = \frac{Nu - Nu_{ref}}{Nu_{ref}} \tag{15}$$

In Figure 2 the relative error (ε_r) in Nu as a function of the number of the grid elements (N) for β = 0.1 and for different values of the Knudsen and Brinkman numbers, is presented. It is evident that for a number of elements N higher than 2000 the value of the relative error tends to 0 which means that the numerical solution becomes independent on the grid resolution. The same trend has been also observed for the other values of the aspect ratio, therefore in all the numerical runs a grid consisting of at least 2000 elements has been adopted.

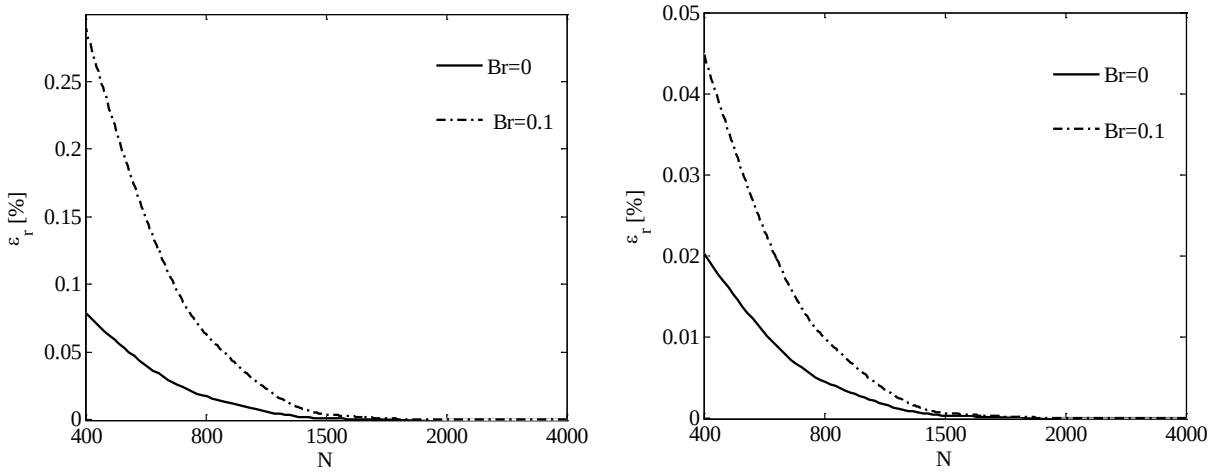

(a) (b)

Figure 2. Relative error in Nusselt number as a function of the grid elements for different values of the Brinkman number: (a) Continuum flow (Kn=0); (b) Slip flow (Kn=0.1).

The validation of the numerical procedure has been performed by comparing the numerical results with the data available in literature. For circular microducts (β =1) an excellent agreement with the analytical values of the Nusselt number obtained by applying the solutions proposed by Aydın and Avcı [5] and by Jeong and Jeong [6] has been found for all values of the Knudsen and Brinkman numbers analysed, as shown in Table 1. The maximum discrepancy between the numerical Nu and the analytical ones is less than 1e-05.

To validate the numerical solution for the elliptical microchannels as well, a comparison between the present numerical results of the Nusselt number for Br =0 and other numerical values available in literature [2, 21] has been performed; as shown in Table 2; a perfect agreement has been found even in this case.

Both benchmarks confirm that the numerical procedure adopted in the present analysis can be considered robust and accurate.

To investigate the influence of the viscous dissipation and rarefaction degree in the considered cross-section, several numerical runs have been performed by considering different values of the main parameters that influence the fluid behavior.

Table 1. Comparison between numerical Nusselt numbers for circular ducts (β=1) and analytical ones.

	Br									
	0		0.005		0.01		0.05		0.1	
Kn	[5] [6]	Present work	[5] [6]	Present work	[5] [6]	Present work	[5] [6]	Present work	[5] [6]	Present work
0	4.364	4.364	4.271	4.271	4.181	4.181	3.582	3.582	3.038	3.038
0.02	4.071	4.071	4.017	4.017	3.964	3.964	3.589	3.589	3.209	3.209
0.04	3.749	3.749	3.717	3.717	3.685	3.685	3.449	3.449	3.194	3.194
0.06	3.439	3.439	3.419	3.419	3.399	3.399	3.248	3.248	3.078	3.078
0.08	3.156	3.156	3.143	3.143	3.130	3.130	3.031	3.031	2.916	2.916
0.10	2.904	2.904	2.895	2.895	2.887	2.887	2.820	2.820	2.741	2.741

Table 2. Comparison between numerical Nusselt numbers for elliptic cross-section and data available in literature for *Br*=0.

	Kn								
	0			0.04		0.06		0.1	
β	[2]	[21]	Present work	[21]	Present work	[21]	Present work	[21]	Present work
0.100	0.6562	0.656	0.656	0.710	0.710	0.720	0.720	0.724	0.724
0.125	0.9433	0.943	0.943	0.999	0.999	1.003	1.003	0.988	0.988
0.200	1.820	1.820	1.820	1.811	1.811	1.768	1.768	1.655	1.655
0.250	2.333	2.333	2.333	2.246	2.246	2.161	2.161	1.973	1.973
0.333	3.006	3.006	3.006	2.778	2.778	2.627	2.627	2.331	2.331
0.500	3.802	3.802	3.802	3.362	3.362	3.121	3.121	2.678	2.678
0.667	-	4.171	4.171	3.618	3.618	3.332	3.332	2.832	2.832
0.750	-	4.266	4.266	3.683	3.683	3.385	3.385	2.868	2.868
0.833	-	4.325	4.325	3.723	3.723	3.417	3.417	2.889	2.889

With regards to the aspect ratio of the elliptic cross-section, the investigation has been carried out assuming the most common values of the aspect ratio, namely β = 0.10, β = 0.125, β = 0.20, β = 0.25, β = 0.333, β = 0.50, β = 0.667, β = 0.75, β = 0.833 and β = 1. It has to be pointed out that to keep the same value of the hydraulic diameter, for each value of aspect ratio both the semi-minor axis (*b*) and the semi-major axis (*a*) have been varied. The role of the viscous forces in the convective heat transfer has been investigated by varying the Brinkman number in the range 0÷0.1 while the rarefaction effects have been taken into account by changing the Knudsen number from 0 (continuum flow) up to 0.1.

In Figure 3 the dimensionless fluid temperature as a function of the semi-minor axis of the ellipse (y) is depicted, for a shallow elliptical channel (β=0.1), for different values of the Brinkman number, namely *Br* =0.005, *Br* =0.01, *Br* =0.05 and *Br* =0.1, and for both continuum flow (*Kn* =0) and slip flow (*Kn* =0.1). It has to be pointed out that in H2 boundary conditions the temperature distribution is calculated apart from an arbitrary constant; the here presented results have been obtained by considering that the dimensionless temperature at the centre of the cross-section is zero. By observing Figure 3a, it can be noticed that the thermal fluid behavior is significantly affected by the viscous heating, when the rarefaction effects are disregarded (*Kn* =0); as the Brinkman number increases from 0.005 to 0.1, the maximum of the non-dimensional fluid temperature, reached at the wall, increases by about 80%. On the contrary the influence of the viscous heating on the fluid behavior becomes less relevant in slip flow regime. It has been observed that as the rarefaction effects become more pronounced the influence of the Brinkman number is reduced. This effect is due to the presence of the slip velocity at the wall which leads to a reduction of the velocity gradient. This trend is evident in Figure 3b in which the non-dimensional temperature profiles as a function of the shorter axis of the

ellipse for *Kn* =0.1, are presented. An increase in the Brinkman number from 0.005 to 0.1 leads an increase in the wall dimensionless temperature of about 19%.

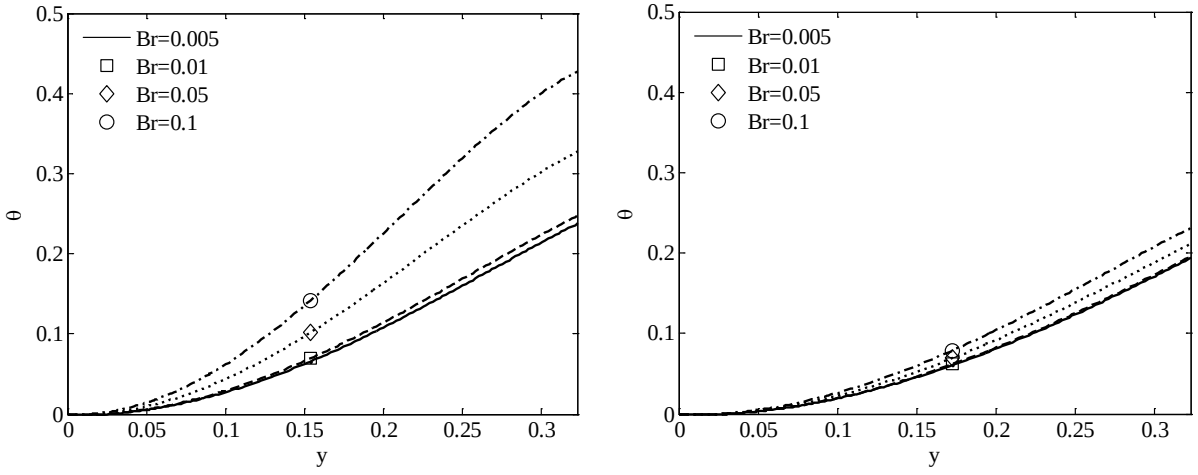

(a) (b)

Figure 3. Non-dimensional temperature profile for β =0.1: (a) Continuum flow (*Kn*=0); (b) Slip flow (*Kn*=0.1).

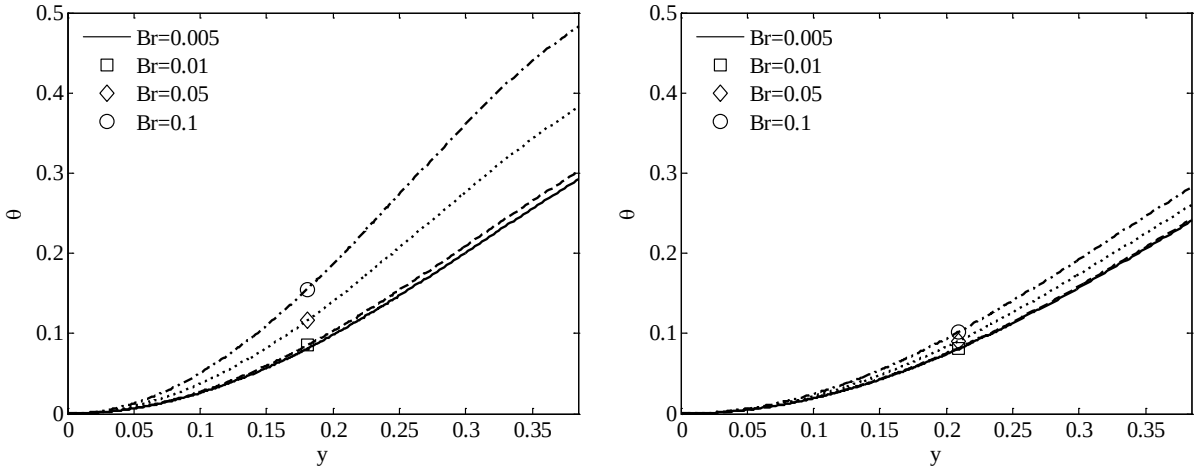

(a) (b)

Figure 4. Non-dimensional temperature profile for β =0.5: (a) Continuum flow (*Kn*=0); (b) Slip flow (*Kn* =0.1).

The same trends have been observed for each value of the aspect ratio considered in the present analysis. Figure 4 shows the non-dimensional temperature profiles for β =0.5, keeping the same values of the Brinkman and Knudsen numbers. However by comparing the graphs presented in Figure 3a with those in Figure 4a, it can be noticed that the influence of the Brinkman number becomes less pronounced as the aspect ratio increases. In fact by increasing *Br* from 0.005 up to 0.1 the dimensionless wall temperature increases by about 65%. On the contrary, within the slip flow regime the influence of the aspect ratio becomes less relevant (i.e. for *Br* changing from 0.005 to 0.1, the wall temperature increases by about 17%).

The influence of the aspect ratio is more evident by observing the graphs shown in Figures 5 and 6. In Figure 5 the Nusselt number as a function of both Knudsen and Brinkman numbers is depicted for several values of the aspect ratio. With regards to the effect of the viscous heating, numerical results have pointed out that viscous dissipation degrades the heat transfer: the Nusselt number decreases as the Brinkman number increases for all values of the Knudsen number and of aspect ratio investigated

in the present study. Similar trends have been also observed by other researchers in different geometry cross-sections (see for instance Tunc and Bayazitoglu [4], Aydın and Avcı [5] and Jeong and Jeong [6] for circular ducts, van Rij et al.[14] for rectangular microducts and Kuddusi [17] for trapezoidal microchannels).

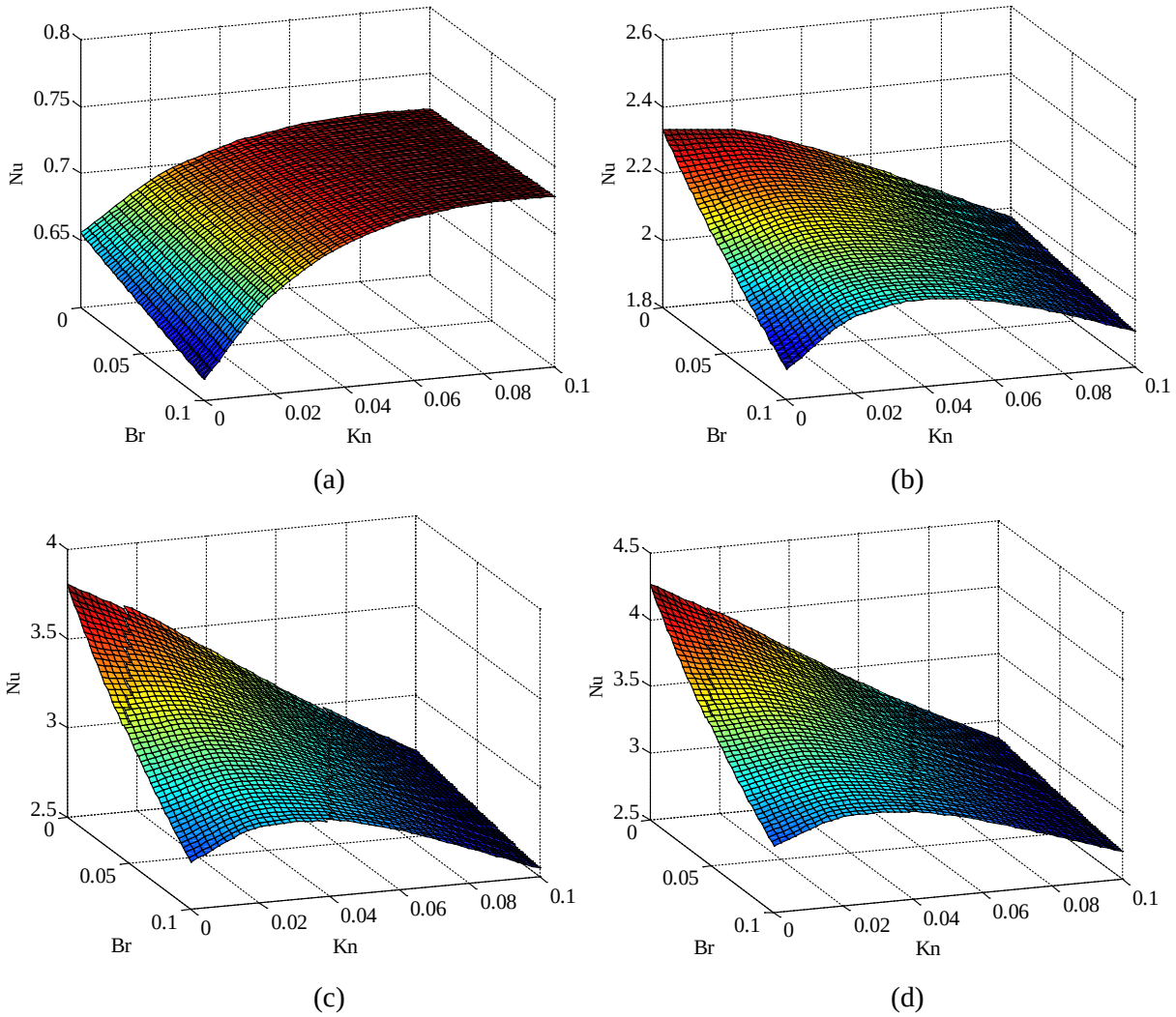

Figure 5. Nusselt number as a function of Knudsen and Brinkman numbers for several values of aspect ratio: (a) β=0.1; (b) β=0.25; (c) β=0.5; (d) β=0.75.

On the other hand the rarefaction effects may increase or decrease the Nusselt number depending on the value of the aspect ratio and of the Brinkman number. In fact for $\beta \geq 0.25$ and for low values of the Brinkman number (i.e. *Br* ranges between 0.01 and 0.04, depending on the value of the aspect ratio), Nusselt number decreases as the Knudsen number increases, while for $\beta \geq 0.25$ and for high values of the Brinkman number, Nusselt number presents a maximum for *Kn* ranging between 0.02 and 0.04 (depending on the values of β and *Br*).

For shallow microchannels the Nusselt number presents a maximum for all values of the Brinkman number considered in the present work; the value of the Knudsen number in which the maximum *Nu* occurs depends on the value of β and *Br*, as it can be noticed by observing Figures 5a and 5b. However, it is important to highlight that for very shallow elliptical microchannels the Nusselt number becomes lower than 1, which means that the convective heat transfer is less efficient than pure heat conduction.

To highlight the influence of the viscous dissipation on the heat transfer coefficient, a comparison between the Nusselt number obtained for $Br > 0$ and the corresponding values for $Br = 0$ computed by Vocale et al. [21], has been performed.

The value assumed by the normalized Nusselt number (i.e. $Nu_N=Nu_{Br>0,Kn>0}/Nu_{Br=0,Kn=0}$) as a function of the aspect ratio β is shown in Figure 6 by taking several values of the Brinkman and Knudsen numbers.

The analysis of the trends of the normalized Nusselt number (Nu_N) leads to the same conclusions as regards the combined effect of the rarefaction and the viscous dissipation, highlighting the influence of the aspect ratio. In fact by observing Figure 6 it can be noticed that for all values of the Knudsen and Brinkman numbers considered in this work, the influence of the viscous dissipation increases as the aspect ratio increases. Values of the normalized Nusselt number larger than 1 can be obtained in the slip flow regime for shallow elliptical channels (β <0.2); the maximum increase of the Nusselt number is obtained for β=0.1 when the rarefaction effects are more evident (Kn=0.1) and this increase is of the order of 10% independently from the value assumed by the Brinkman number. On the contrary, when the elliptic cross section tends to the circular geometry the normalized Nusselt number is always less than 1, which means that both rarefaction and viscous dissipation make worse the convective heat transfer, reducing the Nusselt number by about 30% for β =1 (i.e. circular microducts).

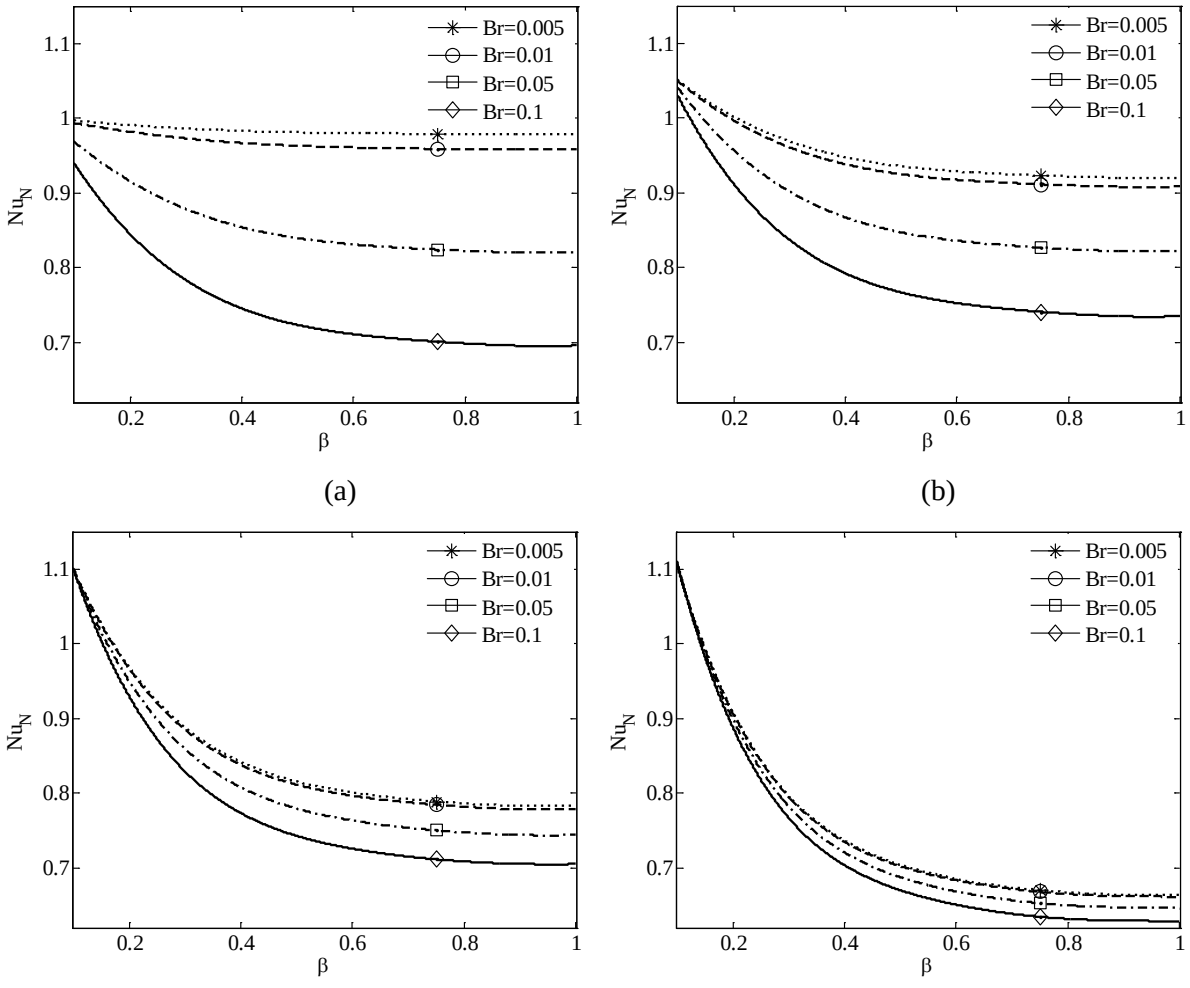

Figure 6. Normalized Nusselt number as a function of the aspect ratio for several values of the Brinkman number: (a) Kn=0 (continuum flow); (b) Kn=0.02; (c) Kn=0.06; (d) Kn=0.1.

4. Conclusions

In this work the role of the viscous dissipation on the convective heat transfer for a laminar and fully developed gaseous flow, in elliptic microducts, has been numerically investigated. The governing equations, which have been solved within the Comsol Multiphysics® environment, have taken also into account the presence of rarefaction effects. The thermal problem has been tackled by considering a constant and uniform heat flux at the wall.

The numerical results, validated against the data available in literature for circular and elliptical cross-sections, show that the viscous forces play a leading role in the convective heat transfer. In particular for high values of the aspect ratio and rarefaction degree, neglecting the viscous dissipation effect may lead to an overestimation of the Nusselt number up to about 59%.

It has been demonstrated that for shallow elliptical microchannels with an aspect ratio β lower than 0.2 the presence of rarefaction effects is beneficial for convective heat transfer and an increase of the Knudsen number determines an increase of the Nusselt number up to 10%. However, it is important to highlight that shallow elliptic channels having an aspect ratio lower than 1/8 are characterized by Nusselt numbers lower than 1 in fully developed laminar regime which means that, even in the case in which rarefaction effects and viscous dissipation effects are negligible, forced convection is ineffective with respect pure heat conduction.

These results confirm that reducing the channel size is not enough to enhance the convective heat transfer coefficient; in fact the viscous dissipation effects shall offset the gains of high heat transfer coefficients associated with a reduction in the channel size.

Acknowledgments

This work has been carried out thanks to the financial support of the PRIN2009TSYPM7_001 project “Single-phase and two-phase heat transfer for microtechnologies. Heat transfer and fluid flow in microscale”.

References

[1] Herwig H and Hausner O 2003 *Int. J. Heat Mass Tran.* **46** 935-937
[2] Shah RK and London AL 1978 *Laminar flow forced convection in ducts* ed Academic Press (New York) chapter III
[3] Colin S 2012 *ASME J. Heat Transf.* **134** 020908
[4] Tunc G and Bayazitoglu Y 2001 *Int. J. Heat Mass Tran.* **44** 2395–2403
[5] Aydın O and Avcı M 2006 *Int. J. Heat Mass Tran.* **49** 1723-1730
[6] Jeong HE and Jeong JT 2006 *J.Mech. Sci Technol.* **20** 158-166
[7] Çetin B, Yazicioglu AG and Kakac S 2009 *Int. J. Therm. Sci*. **48** 1673-1678
[8] Sun W, Kakac S and Yazicioglu AG 2007 *Int. J. Therm. Sci*. **46** 1084-1094
[9] Hooman K 2007 *Int. J. Heat Mass Tran.* **34** 945-957
[10] Sadeghi A and Saidi MH 2010 *J Heat Transf.* **132** 072401
[11] Jeong HE and Jeong JT 2006 *Int. J. Heat Mass Tran.* **49** 2151-2157
[12] Aydın O and Avcı M 2007 *Int. J. Therm. Sci*. **46** 30-37
[13] Zhang T, Jia L, Yang L and Jaluria Y 2010 *Int. J. Heat Mass Tran.* **53** 4927-4934
[14] van Rij J, Ameel T and Harman T 2009 *Int. J. Therm. Sci*. **48** 271-281
[15] van Rij J, Ameel T and Harman T 2009 *Int. J. Heat Mass Tran.* **52** 2792-2801
[16] Sun Z and Jaluria Y 2012 *Int. J. Heat Mass Tran.* **55** 3488-3497
[17] Kuddusi L 2011 *Int. J. Heat Mass Tran.* **54** 52-64
[18] Karniadakis G, Beskok A and Aluru N 2005 *Microflows and Nanoflows – Fundamentals and Simulation* ed Springer (New York) chapter 2
[19] Morini GL, Spiga M and Tartarini P 2004 *Superlattice Microst.* **35** 587-599
[20] Spiga M and Vocale P 2012 *Adv.Mech. Eng.* **2012** 481280
[21] Vocale P, Morini GL and Spiga M 2014 *Int. J. Heat Mass Tran.* **71** 376-385